Nat Hazards (2012) 62:1169–1189
DOI 10.1007/s11069-012-0142-4

ORIGINAL PAPER

Synoptic forcing of wave states in the southeast Chukchi Sea, Alaska, at an offshore location

Oceana P. Francis · David E. Atkinson

Received: 26 September 2011 / Accepted: 9 March 2012 / Published online: 31 March 2012

Abstract A bottom-mounted Recording Doppler Current Profiler was placed at an offshore location (depth of 34 m) in the southeast Chukchi Sea, Alaska, from July through December 2007 (UTC) with the objective of linking observed wave activity—wind-sea and swells—to their synoptic drivers. A total of 47 intervals of elevated wave state were recorded: 29 exceeding 1 m significant wave height (SWH), 16 exceeding 2 m SWH, and 3 m exceeded on two occasions; during one of those, a SWH of 4 m was observed. Detailed analysis of the two large events, including comparison with high-resolution reanalysis wind data (North America Regional Reanalysis), showed wave direction from the east, varied about 15° to the north (counterclockwise) from the wind direction, and current flow in the opposite direction (from the west). This is thought to be the influence of a strong "wind-sea" presence. Regarding classic wave limitations, although the SE Chukchi Sea is a large embayment bordered by land to the east, fetch limitations from the northeast and southeast did not appear to be a constraint for the wind speeds indicated by reanalysis. These two events appeared to be driven by winds associated with cyclonic systems that moved into the eastern Bering Sea and stalled. Examination of smaller waves associated with these events suggested that waves of 1.5 m SWH or less are likely part of another regime and can either be swell or wind-sea, moving in from the open Chukchi Sea to the northwest or through the Bering Strait to the south.

Keywords Offshore · Waves · Wind · Storms · Recording Doppler Current Profiler · Chukchi Sea · Bering Sea · Delong Mountain transportation system

O. P. Francis (✉) · D. E. Atkinson
Department of Atmospheric Sciences, International Arctic Research Center, University of Alaska Fairbanks, PO Box 757340, Fairbanks, AK 99775, USA
e-mail: oceana@iarc.uaf.edu

D. E. Atkinson
e-mail: datkinso@uvic.ca

Present Address:
D. E. Atkinson
Department of Geography, University of Victoria, PO Box 3060, STN CSC, Victoria, BC V8W 3R4, Canada

1 Introduction

Severe wind-generated sea states affect most users and inhabitants of coastal regions: shipping operations, coastal communities, engineering considerations, and planners. Coastal western Alaska (Chukchi and Bering Seas—Figs. 1, 2) is particularly vulnerable to severe wave states. Although the quantity of infrastructure in this area is limited, it is typically critical for the communities served. The coastal area is vulnerable to storm events because of the low elevation and residents living in close proximity to the water. The remoteness of this region means damages to coastal infrastructure are difficult and costly to repair due to the expense of shipping materials and crews into the area and the limited construction season. In the last 17 years, a decrease in sea ice cover (i.e., interannual variations of local shore-fast ice and the multiyear ice pack) has increased fetch and the duration of open-water season (Francis et al. 2011). The decrease in ice cover combined with large synoptic-scale extreme storm events that pass through the area increases the potential for major damage. For example, there has been an increase in coastal erosion at communities in this region such as Kivalina where several meters of shoreline are usually lost from a single storm event (USACE 2003, 2004). A major industrial stakeholder in this area is Teck Alaska Inc., who operates the Delong Mountain Terminal. This facility has experienced periods when waves have caused shutdowns due either to direct impact on the terminal infrastructure or to set up of dangerous conditions for handling the large freighters, which given their length (up to 300 m) can be especially susceptible to wave action. Finally, wave climatologies and their results impact engineers and planners who must design for the maximum anticipated loads on infrastructure; the highest magnitude impact on coastal infrastructure in terms of kinetic energy is often due to wave action. In each of these cases, the limited knowledge of wave state and its atmospheric linkages in this region impedes arriving at a balance between cost-effectiveness and safety for coastal engineering structures. Further, this area is presently experiencing increased activity

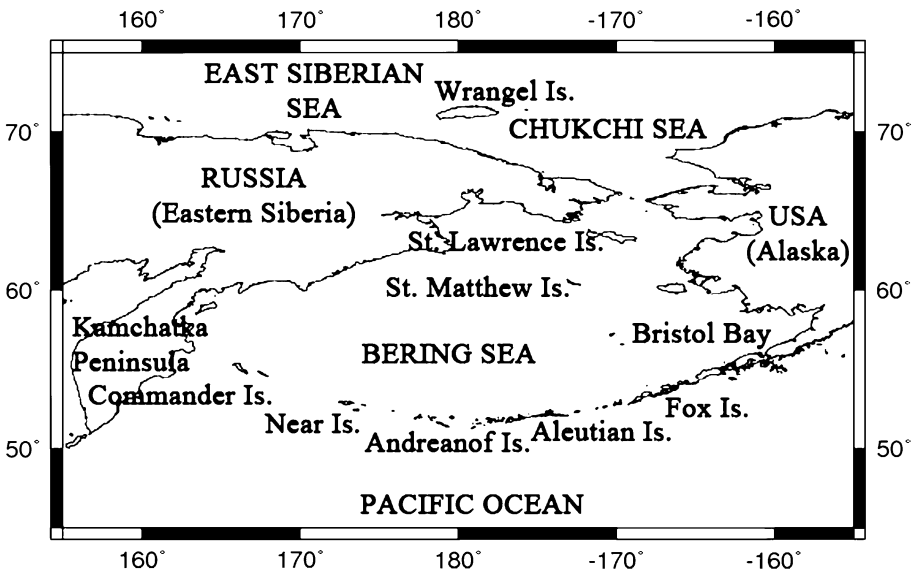

Fig. 1 Geographical map of East Siberia/Alaska

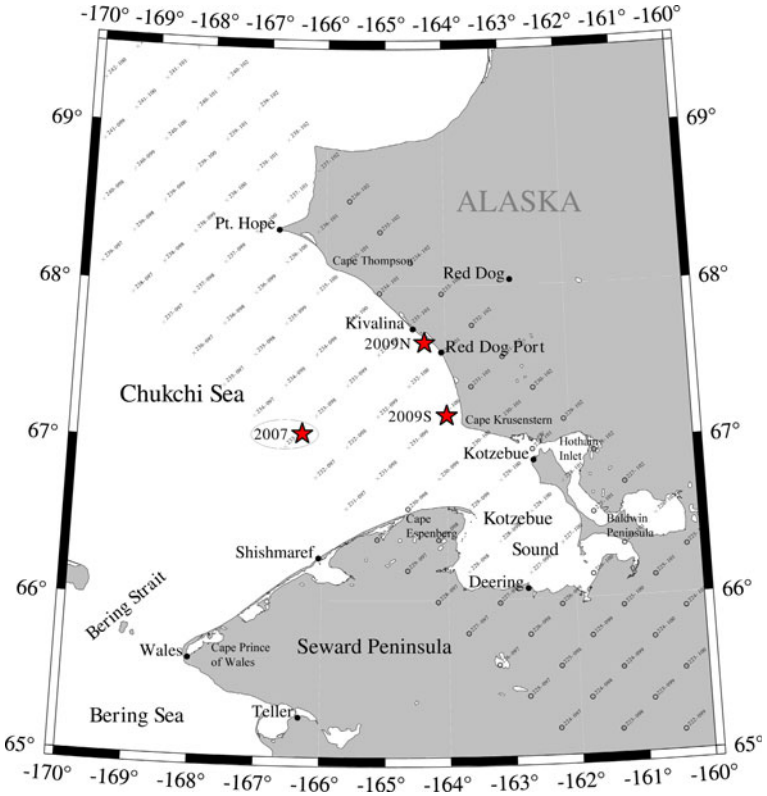

Fig. 2 In situ measurement locations in the Chukchi Sea. Geographical map of southeastern Chukchi Sea showing location of NARR 10 m winds (small print—for location purposes only) and the three RDCP Stations 2007 (mentioned in this paper, offshore—"*circled star*"), 2009N, and 2009S (*stars*) (mentioned in Francis and Atkinson 2012—for the nearshore)

associated with interest in oil development. Thus, to improve design and operational resilience, there is a longstanding need to improve our understanding of the specific linkages between atmospheric forcing and the resultant sea state. Therefore, there is a particular interest in the wave regime in the Chukchi Sea. Using an observational wave data set from (RDCPs), this paper focuses on the occurrence of waves and their associated synoptic drivers in the SE Chukchi Sea. Specifically, the focus is identifying drivers of "wind-sea" (i.e., waves under influence of wind) versus those causing "swell" (i.e., waves moved away from wind generating area, and not under influence of wind).

The focus in this study is significant wave height (SWH), as high-magnitude winds are directly correlated to wave heights. SWH is the highest 33 % of wave heights in the wave record. The SWH depends primarily on fetch (the distance over which the wind blows), wind speed (commonly measured at the 10 m elevation), and the duration of the wind. Wind speed of greater magnitude results in greater wave height. The duration, which is the time the wind blows in one direction, results in greater wave height, the longer the duration. The fetch, which is the distance the wind blows in one direction, results in greater wave height, the longer the fetch. In a fully developed sea, maximum fetch and maximum duration are reached, and SWH solely becomes the function of wind speed.

The primary objective of this study is to identify and characterize the synoptic and meso-scale patterns that drive observed occurrences of SWH events in the southeast Chukchi Sea. A secondary objective is to distinguish between the occurrence of swells and wind-sea. A third objective is to assess the extent to which wind data extracted from a widely used, high-resolution reanalysis data set (NCEP North America Regional Reanalysis) is correlated to the observed wave conditions found in the RDCP wave data set and thus its suitability for longer-term modeling of wave forecasting and hindcasting in this region. Although it is known that reanalysis winds tend to underestimate peak storm wind speeds (Swail and Cox 2000), especially the large spatial-scale global reanalyses, what this means specifically for reproducing waves in the southeast Chukchi is not precisely known. These tasks will utilize observational data acquired from RDCPs placed in the southeast Chukchi Sea in 2007. Estimates of observed SWH event occurrences will be generated using data from the 32-km resolution "North American Regional Reanalysis (NARR)" atmospheric data set (Mesinger et al. 2006) and the NCEP/DOE Global Reanalysis 2 (Kistler et al. 2001). It is hypothesized that, in the SE Chukchi Sea study area, the primary wave direction is from the northwest because that is the direction of greatest fetch, and the land formation around the Bering Strait allows minimal Bering Sea swell to propagate through. These factors are elaborated upon below.

The organization of the paper consists of an overview of the regional atmospheric setting and instrumentation background and a results section describing major observed wave events with detailed analysis and intermediate conclusions. Broader conclusions and discussion are provided in the discussion section. It was felt that it would be more efficient to analyze the wave events as they were described, for clarity.

2 Background

2.1 Atmospheric circulation and synoptic conditions

The synoptic situation governing the Bering and Chukchi Seas in the July through December time frame is dominated by transient low-pressure systems—"storms"—moving into the region from the North Pacific. Mesquita et al. (2010) conducted a seasonal analysis of storm properties in this region, including frequency. Their work showed higher levels of various indicators of storm activity in the fall and winter seasons, including frequency, intensity, and track speed. Most storm systems do not form locally, but move into the region when upper-level winds are favorable. The more typical end point for these North Pacific systems is the Gulf of Alaska, a favored end location; however, the Bering Sea is also a common end point. One aspect of the location of the Bering Sea with respect to the typical position of the jet stream, especially in fall/winter/early spring, is that storm systems can often stall in the eastern Bering Sea, where they linger until they infill and dissipate. In some cases, storms moving into the Bering Sea transit the Bering Strait and move up into the Chukchi Sea area. A secondary storm pathway—"northern" storms—runs roughly east to west across the north Russian/Alaska coast.

Most of these storms are extra-tropical cyclones. These large weather systems (1,000s of km in extent) in general depend on baroclinic atmospheric conditions, which explains their greater frequency in the non-summer period (Mesquita et al. 2010). The most powerful systems, which can attain central mean sea level pressures (MSLPs) down into the 930 hPa range with winds of +100 knots, form under less-common conditions when large

quantities of water vapor are available in the mid-troposphere and dynamical support is available in the form of a suitably situated upper-air trough.

Wave conditions generated by these systems may be categorized into several broad groups. Bering Sea storms, depending on their track and position, produce an easterly to southeasterly local wind flow across the SE Chukchi Sea region. If the storm center is situated farther to the west, the winds can be southerly. These prevailing wind directions generate corresponding wind-sea in the SE Chukchi, and there is the potential for swell to be transmitted northwards through the Bering Strait, which may be more readily observed if the storm is positioned farther south and the wind-sea regime is weaker. Northern storms generate southeast winds and wave directions over this region. All of this is mitigated by the yearly development of shore-fast ice. During the part of the year when most of the Chukchi Sea is open water, strong winds from northern storms can operate over considerable fetch (hundreds of km), driving waves to the southeast into the SE Chukchi region.

2.2 Site selection and RDCP instrument deployment

The observational location in southeast Chukchi Sea was chosen for several reasons: little work has been done north of the Bering Strait on the synoptic driving of sea states, the area has demonstrable strong wave forcing (Jensen et al. 2002) and possesses an interesting and complex regime that can include wind-sea and swell (Jensen et al. 2002), and there are various at-risk coastal inhabitants (several villages and an industrial operator).

The overall project entailed three data-gathering efforts using RDCP deployments. One RDCP was deployed to an open-water location (34 m depth) during the ice-free period, July through December 2007 UTC ("2007" in Fig. 2), discussed in this paper, and two RDCPs were later deployed to coastal locations during ice-free and ice-covered periods October 2009 through September 2010 UTC ("2009 S" and "2009 N" in Fig. 2, depth of 17 and 18 m, respectively), discussed in a forthcoming paper.

3 Methods and data

For this study, wind and wave direction are taken to be of the same convention. Wind direction is defined as the direction *from which* the wind is coming and is given in degrees true bearing. Current direction is defined as the direction *to which* the current flow is going toward in degrees true bearing. The *true bearing* to a point is the angle measured in degrees in a clockwise direction from the north line.

3.1 Atmospheric data sets

Atmospheric parameters were obtained from the "NARR" data set (Mesinger et al. 2006). This gridded data of 0.3° and 1° resolution are taken from data-assimilative fluid-dynamic model. This system, a "reanalysis" data set, was developed and is maintained by the National Centers for Environmental Prediction (NCEP) of the US National Oceanic and Atmospheric Administration (NOAA). For this project, three parameters were extracted from the NARR data set—geopotential height at 925 hPa, vector wind at 925 hPa, and vector wind at 10 m. Storm center, position, and tracking were evaluated using geopotential height at 925 hPa and vector wind at 925 hPa. Local winds were evaluated using vector wind at 10 m and extracted as time series from the NARR grid point nearest to the RDCP instrument location (Fig. 2 for NARR grid point locations). MSLP data from the

NCEP/National Center for Atmosphere Research Global Reanalysis data set (Kistler et al 2001) were also used in this analysis.

3.2 RDCP wave parameters

The bottom-positioned RDCP (AADI 2006), by analyzing Doppler shifts of acoustic returns, recorded a number of wave observations denoted here as N. The sampling frequency of the RDCP is 2 Hz. A given N is a reduction of 15 min of individual wave observations $i = 1{,}800$ samples; this cycle occurs every time the RDCP awakens, which was once every 2 h. Station 2007 conducted one of set 15-min measurements every 2.0 h, resulting in 3,816 h and 6-min total recording time, so the number of wave observations was $N = 1{,}704$. Each observation i includes wave height H_i, wave period T_i, and wave direction D_i. From these parameters, the RDCP estimates the following: SWH, H_{m0}, mean wave period, T_{m01}, mean zero-crossing, T_{m02} *or* $\bar{T}_z$, energy wave direction, D_E, mean direction, D_m, and peak direction, D_p. For this study, SWH, H_{m0}, mean zero-crossing, T_{m02}, and mean wave direction, D_m were retained for analysis. The mean zero-crossing parameter, T_{m02}, is the time obtained by dividing the record length by the number of down crossings (or up crossings) in the record (AADI 2006), compared to the mean wave period, T_{m01}, which is the wave period corresponding to the mean frequency of the spectrum (WMO 1998). Figure 3 shows a graphical representation of how the mean zero-crossing parameter, T_{m02} is calculated—from the individual zero-crossing wave period, T_i, where the individual wave height, H_i, performs a zero-upcrossing (red circles).

Wave spectra were estimated using the maximum likelihood method (MLM). Upper cutoff frequency was 0.6 Hz. Fast Fourier transform (FFT) size was 128.

3.3 Wave event and atmospheric analysis

A "significant wave height" event (SWH) was defined along the lines of similar approaches used in Hudak and Young (2002) and Francis-Chythlook (2004); that is, the wave magnitude exceeds and remains over a given threshold for a period of 6 h or more in duration. Three threshold set points were established: 1, 2, 3 m. The SWH event was considered to have ended when the wave magnitude dropped below the threshold for 6 h or more.

Spatial plots of pressure and winds were manually examined to assess the atmospheric state at the time of identified SWH events. The atmospheric forcing typically was a "storm" as defined by the existence of a closed low feature on a 925 hPa. However, persistent patterns consisting of strong pressure gradient that were not storms in transient short wave sense are not uncommon in this region. The 925 hPa level was chosen to minimize interference from surface conditions, yet provide a level low enough to adequately represent surface pressure conditions.

4 Station 2007 results

4.1 Station 2007 overview

In the July–December 2007 recording period, forty-seven (SWH) events were identified: twenty-nine 1 m, sixteen 2 m, and two 3 m. The longest duration events occurred in two

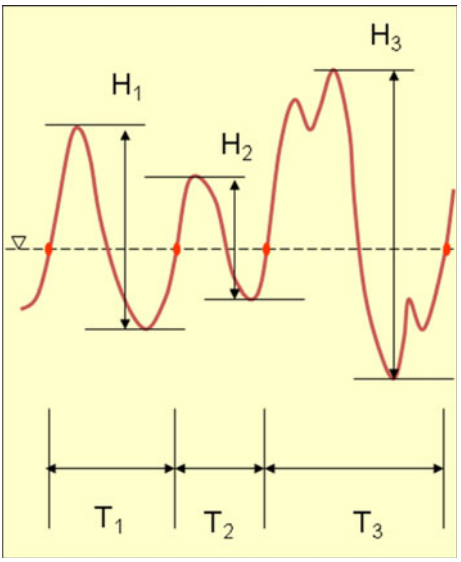

Fig. 3 Representation of wave height and zero-crossing period. Graphical representation of individual wave height, H_i, and the corresponding individual zero-crossing wave period, T_i. Mean zero-crossing parameter, T_{m02}, is calculated from the individual zero-crossing wave period, T_i, where the individual wave height, H_i, performs a zero-upcrossing (*red circles*)

distinct periods: mid-September to mid-October and November to early December. The longest duration/large magnitude events (2 and 3 m events) occurred in late November to early December. The SWH (Fig. 4) for July–December 2007 encompasses the entire RDCP Station 2007 wave record. The NARR 10-m wind speed (Fig. 5) also for July–December 2007 is shown to correlate well with the SWH (Fig. 4), especially for wind speeds >6 m s^{-1}. This suggests that the waves are wind-driven.

The RDCP mean wave direction (Fig. 6) for July–December 2007 is shown to arrive from all directions, with the largest number of *N* waves arriving from the westerly and northerly directions. These waves generally had SWHs < 2 m. During July to September, the wave direction was shown to be mainly westerly and northerly where most of the SWHs were less than 1 m. During September to November, the wave direction was mostly northerly and some easterly where SWHs were generally between 1 and 2 m. During December, westerly and northerly wave directions dominated, while SWHs were generally between 1 and 1.5 m.

Sea surface temperature (SST), monitored by Station 2007, dropped and remained below 0 °C starting December 6, 2007. The water temperature can indicate the potential for shore-fast ice development. However, due to the wave activity where a northerly SWH > 2 m was generated from a northerly wind direction >6 m s^{-1} during mid-December (Fig. 4), sea ice was thought to form right after this period.

The NARR 10-m wind direction (Fig. 7) was not correlated to wave direction for SWHs < 1.5 m. However, for SWHs > 2 m (Table 1), the wave and wind directions showed the strongest correlation. The results shown in Table 1 refer to the wave and wind conditions when the SWH $\geq$ 2 m during a particular "event"—where an "event" is described in Sect. 3.3. The two largest SWH events, both 3 m, are examined below in detail: event "SWH-3m-3" known as SWH Event 1 or "SE1" (Table 1), September 18–27, 2007, and event "SWH-3m-15", known as SWH Event 2 or "SE2" (Table 1), November 22–December 2, 2007. For these two events, the wave signal evolution is overviewed, followed by an examination of the lifecycle of the storm or atmospheric

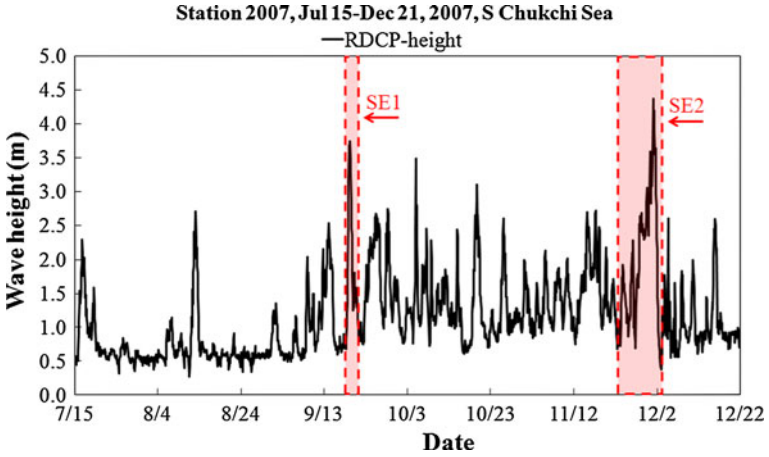

Fig. 4 Station 2007 SWH. RDCP SWH at Station 2007 for entire RDCP wave record July 15–December 21, 2007. Station location and depth are 67°3′29.94″N, 166°20′43.02″W, and 34 m, respectively

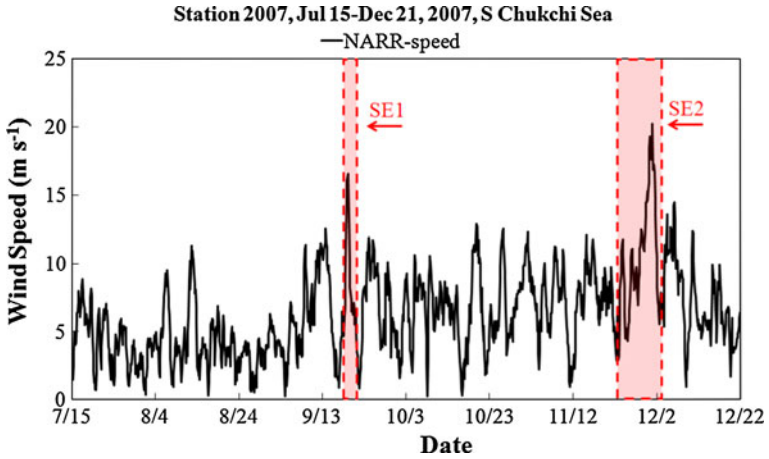

Fig. 5 Station 2007 wind speed. NARR 10-m wind speed at Station 2007 for entire RDCP wave record July 15–December 21, 2007. Station location and depth are 67°3′29.94″N, 166°20′43.02″W, and 34 m, respectively

condition identified as the driving mechanism for the SWH event. Finally, a consideration of near-surface winds at the RDCP location in the context of fetch is presented.

4.2 SE1 (SWH-3m-3), September 18–21, 2007 UTC

SE1 (SWH-3m-3) commenced September 18, 0800 UTC (all times are given in UTC) and ended September 21, 0600, lasting for a total duration of 70 h with SWH in excess of 1 m. In brief, the event proceeded as follows (Fig. 8): rapid initiation and SWH increase from approximately 0.5 to 3.5 m in the first 10 h, maintained the peak wave condition for 16 h, followed by rapid wave height decay to 1.0–1.5 m, and remained at that elevated state for the next 30 h. The directional estimates for this event began with a westerly 1 m SWH

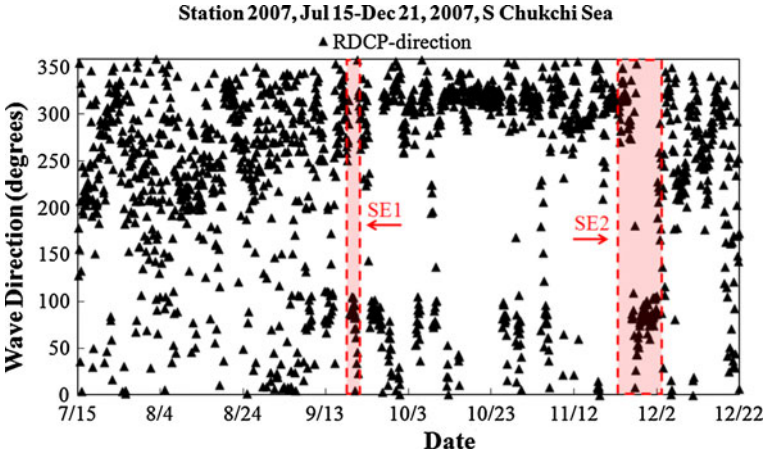

Fig. 6 Station 2007 wave direction. RDCP wave direction at Station 2007 for entire RDCP wave record July 15–December 21, 2007. Station location and depth are 67°3′29.94″N, 166°20′43.02″W, and 34 m, respectively

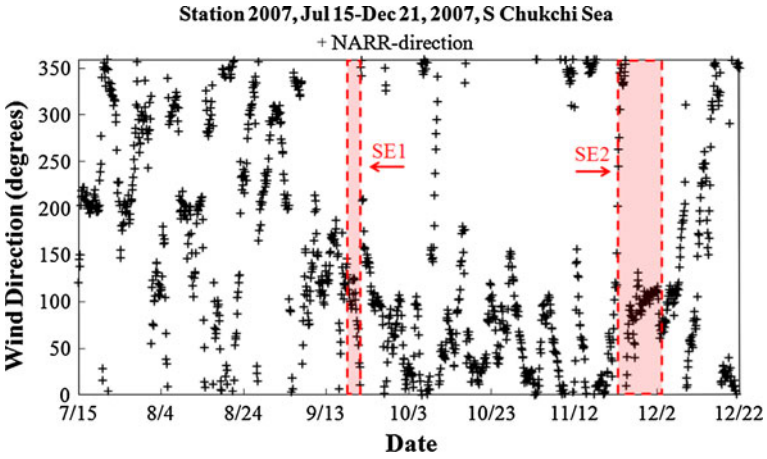

Fig. 7 Station 2007 wind direction. NARR 10-m wind direction at Station 2007 for entire RDCP wave record July 15–December 21, 2007. Station location and depth are 67°3′29.94″N, 166°20′43.02″W, and 34 m, respectively

(Fig. 9) that was maintained for 5 h (September 18, 0800–September 18, 1300). On September 18, 1500, a rapid change in wave direction to easterly occurred. After this change, SWH increased rapidly from 1 to 2 m (also wave period increased rapidly from 4.3 to 5.0 s). For the next 54 h (September 18, 1500–September 20, 2100), wave direction remained easterly. During this 54-h period, a 3 m SWH was sustained for 16 h (September 18, 1900–September 19, 1100). Following the 3 m SWH period, the SWH decreased to 2 m for 7 h until September 19, 1800. The final 36 h saw a SWH of 1 m ending on September 21, 0600. In the final 9 h (September 20, 2100–September 21, 0600), wave direction changed again, back to westerly.

Table 1 Station 2007 SWH events $\geq$ 2 m. Station 2007 SWH events (2 m-"minor" and 3 m-"major" in *italics* to designate "SE"), (l to r) SWH duration, SWH, wave period, wave direction, fetch, NARR wind speed, and wind direction for wave record July 15, 2007–December 21, 2007 UTC at 67°3′29.94″N, 166°20′43.02″W, water depth 34 m

SWH event	Date	SWH duration (h)	H_{m0} (m)	T_{m02} (s)	Wave dir (deg)	Wind speed (m/s)	Wind dir (degree)
2007-2 m-1	8/12–8/13/2007	18	2.3	4.7	207	10.2	201
2007-2 m-2	9/13–9/14/2007	22.5	2.2	4.8	108	10.4	161
2007-3m-3[a]	*9/18–9/19/2007*	*24.75*	*3.1*	*5.5*	*93*	*13.1*	*106*
2007-2 m-4	9/23–9/26/2007	58.5	2.3	5.1	87	10.2	100
2007-2 m-5	9/28–9/28/2007	15.75	2.5	5.2	57	7.9	80
2007-2 m-6	10/4–10/5/2007	11.25	2.7	5.4	86	8.6	87
2007-2 m-7	10/7–10/7/2007	6.75	2.2	5.0	330	6.8	7
2007-2 m-8	10/14–10/15/2007	6.75	2.3	5.0	19	7.7	99
2007-2 m-9	10/19–10/20/2007	31.5	2.4	5.4	326	11.6	22
2007-2 m-10	10/25–10/26/2007	15.75	2.3	5.1	87	11.7	71
2007-2 m-11	11/15–11/15/2007	22.5	2.4	5.3	294	10.0	351
2007-2 m-12	11/16–11/17/2007	13.5	2.5	5.2	1	9.8	4
2007-2 m-13	11/17–11/18/2007	9	2.3	5.1	91	6.5	12
2007-2 m-14	11/25–11/26/2007	9	2.1	5.0	86	10.6	84
2007-3m-15[b]	*11/27–12/2/2007*	*105.75*	*2.9*	*5.5*	*86*	*14.1*	*104*
2007-2 m-16	12/15–12/16/2007	20.25	2.3	5.4	310	7.5	338

[a] 2007-3m-3 (also known as SE1)

[b] 2007-3m-15 (also known as SE2)

The primary feature of the synoptic situation (Fig. 10) that evolved during the lifespan of SE1 was a storm that occurred over 15–18 September, which appeared to be the source of winds necessary to support the observed wave response. The storm entered the southwestern Bering Sea on September 15, 0000, between Komandorskiye Ostrova (Commander Islands) (Russia) and Near Islands (US) (see Fig. 1 for geographical locations). The pressure gradient was enhanced by the juxtaposition of a high-pressure system to the southeast, over the Gulf of Alaska, resulting in the highest wind speeds in the southeast quadrant of the system. Throughout the day on September 15, the storm moved eastward, positioning itself between Near Islands and Andreanof Islands with wind speeds (925 hPa) increasing to 16 m s^{-1} by 1500. The storm then moved northward, positioning itself between the Andreanof Islands and St. Matthew Island by September 16, 0000 with geopotential height and wind magnitude and direction remaining constant. A drop in geopotential height and an increase in wind speed (925 hPa) began on September 16, 1800 as the storm entered a period of strong intensification. Over the next 9 h, the geopotential height dropped rapidly from 650 to 450 m, and the wind speed (925 hPa) increased from 16 to 35 m s^{-1} as the storm entered its peak intensity phase. Low geopotential height (compared to other locations at the same latitude) indicates the presence of a storm, so the drop in geopotential height signifies the intensification of the storm.

The peak of the storm spanned the period September 17, 0900 to September 19, 0600 (45 h). The 925 hPa geopotential height remained consistently low during this period: 400–450 m. Corresponding winds during this time affected the entire Bering Sea, with the

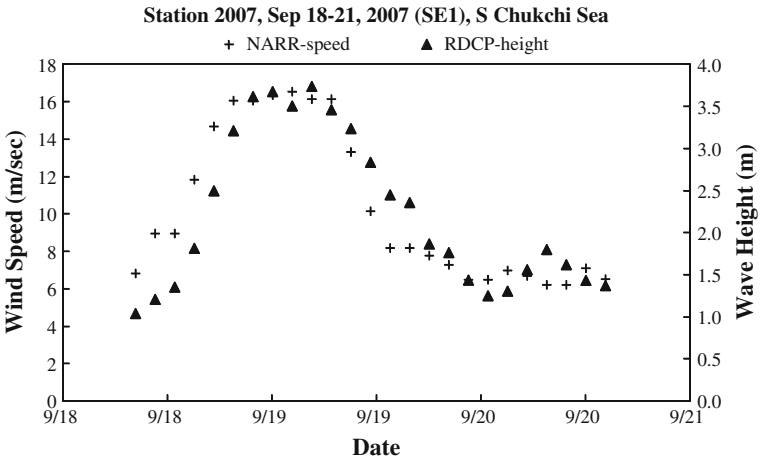

Fig. 8 SE1 wave height versus wind speed. Comparison of RDCP SWH and NARR 10-m wind speed at Station 2007 for wave record September 18–21, 2007 (SE1) at 67°3′29.94″N, 166°20′43.02″W, and a water depth of 34 m

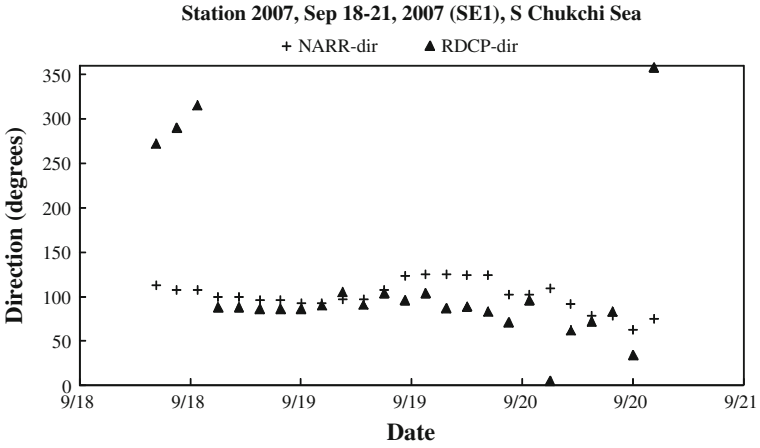

Fig. 9 SE1 wave direction versus wind direction. Comparison of RDCP mean wave direction and NARR 10-m wind direction at Station 2007 for wave record September 18–21, 2007 (SE1) at 67°3′29.94″N, 166°20′43.02″W, and a water depth of 34 m

strongest observed winds over the Andreanof Islands. By this point, storm winds were also affecting southeast Chukchi Sea: easterly winds of approximately 25 m s^{-1} were now in place over Station 2007 (925 hPa). The MSLP for this storm event reached and remained at its minimum of 970 hPa for a 36-h period from September 17, 0900 to September 18, 2100. This time frame encompassed the beginning of SE1. The storm intensity began to wane on September 19, 0600; the period of maximum SWH lasted only a few hours longer. By September 19, 1500, 925 hPa winds over Kotzebue Sound had dropped to 10 m s^{-1}, becoming SSE.

Figure 11 shows the wave spectrum at the highest SWH during September 19, 0400, which was at the end of the peak storm period over the Bering Sea (September 17, 0900–

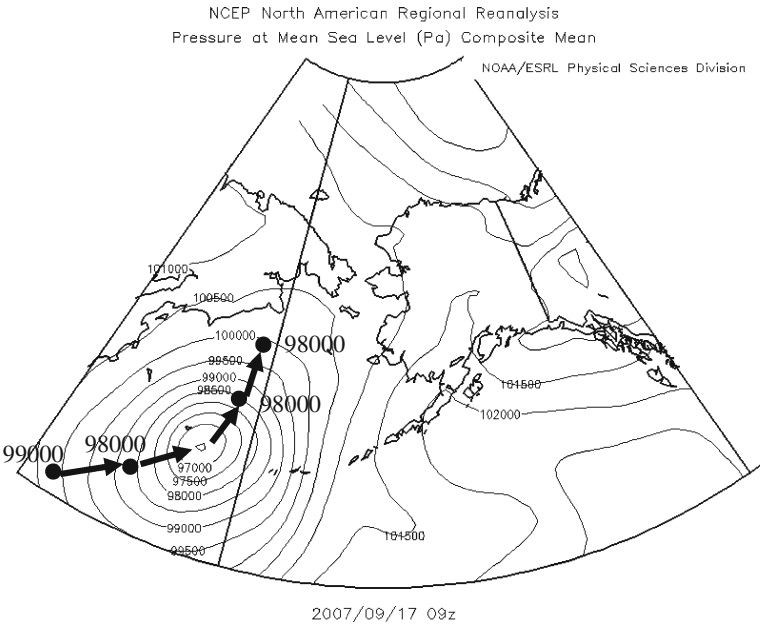

Fig. 10 SE 1 storm maxima. Storm maxima during SE1 on September 17, 2007 0900 UTC shown on (NARR, MSLP) map. Image provided by the NOAA-ESRL Physical Sciences Division, Boulder Colorado at http://www.esrl.noaa.gov/psd. Modified by O. Francis, January 2011

September 19, 0600). This was also a few hours before the highest wind speeds (+16 m s^{-1}) over the SE Chukchi Sea (10 m wind level). The color bar (top) and non-directional (bottom) give the wave energy density, $E(f)$, in m^2Hz^{-1}. The wave-spectra Cartesian contour plot (Fig. 11) shows that the energy is contained in a range of frequencies from 0.10 to 0.15 Hz and a 80° direction range for $E(f) > 2$ m^2Hz^{-1}. The non-directional peak energy density was 14.0 m^2Hz^{-1} (Fig. 13—bottom) at 0.14 Hz, while the directional (Fig. 13—top) was centered at 0.14 Hz coming from 105° (East). The integral wave parameters of this particular spectrum were SWH = 3.7 m, $T_{m02} = 5.8$ s, $T_{m01} = 6.0$ s. The mean winds during the period of the spectrum had a wind speed of $U_{10} = 16.2$ m s^{-1} with wind direction of $U_{\text{dir}} = 97°$. Wind and wave direction were both easterly, where wave direction (105°) was at an 8° clockwise difference from wind direction (97°). The wave phase speed is given by $g/2\pi f_p$ (Ewing 1980), where f_p is the peak frequency or the inverse of the peak period. With the wind speed (16.2 m s^{-1}) and the RDCP peak period, f_p (6.0 s) the wind speed was greater than the wave phase speed (9.4 m s^{-1}). When the wind speed is greater than the wave phase speed, this indicates "wind-sea". When the wind speed is less than the wave phase speed, this indicates "swell". Since the wind speed is much greater than the wave phase speed, this strongly indicates an easterly "wind-sea" for the event of September 19, 0400.

At the beginning of SE1, the wind (at the 10 m level) was ESE at 6 m s^{-1} with its fetch from the vicinity of Cape Espenberg. However, the wave direction was westerly instead of easterly (Fig. 9); that is, opposite to the local wind over the RDCP. By September 18, 1500, this was changing rapidly as the wave direction switched almost 180° to easterly, closely matching the local wind direction. The wind magnitude also increased rapidly at

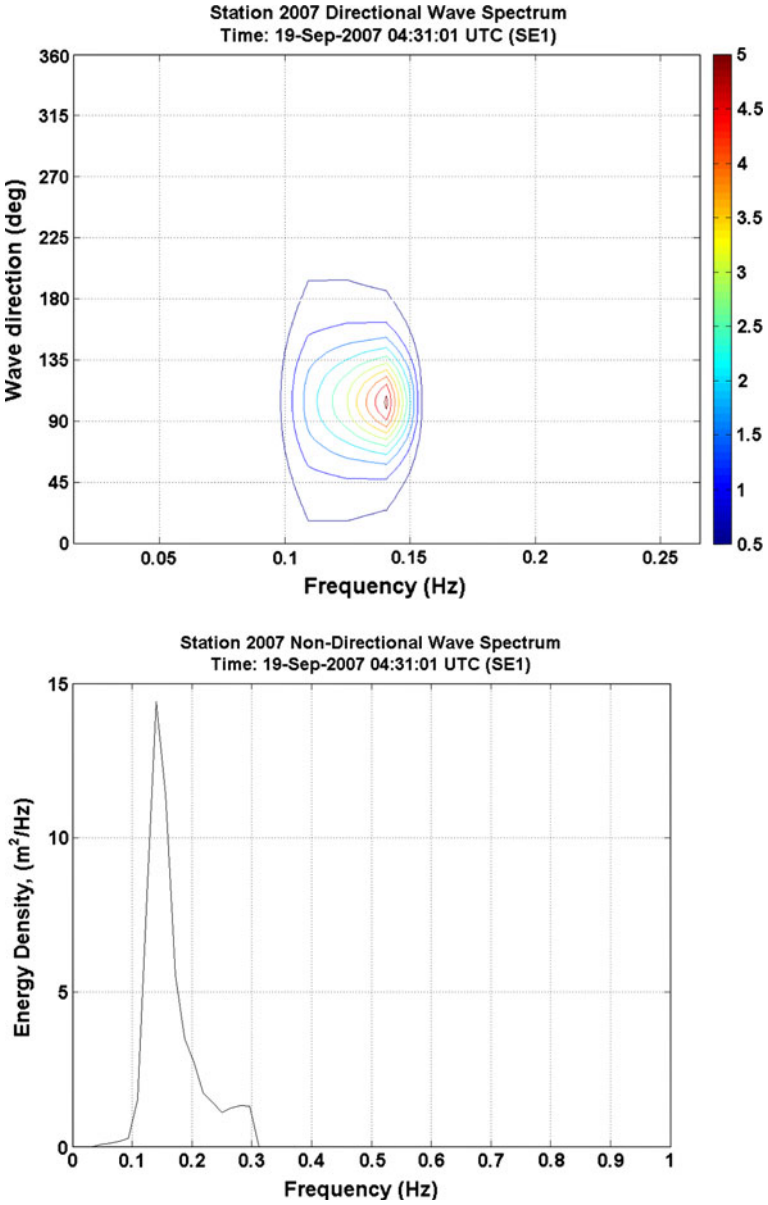

Fig. 11 SE1 wave spectrum. Directional (*top*) and non-directional (*bottom*) wave spectra Cartesian projection of highest SWH in SE1 on September 19, 2007 0431 UTC during SE1, SWH = 3.7 m recorded by the RDCP at Station 2007 at 67°3′29.94″N, 166°20′43.02″W, and with a water depth of 34 m. *The color bar* (*top*) and non-directional (*bottom*) give the wave energy density, $E(f)$, in m^2Hz^{-1}

this time to 9–12 m s^{-1}. Over the next 9 h, surface wind magnitude increased to 16 m s^{-1} at which point 3 m SWHs were observed. Wind and wave directions both remained easterly, although directional consistency began to diverge for wind speeds below 10 m s^{-1} on September 19, 1300; and ultimately for winds less than 8 m s^{-1}, the wind

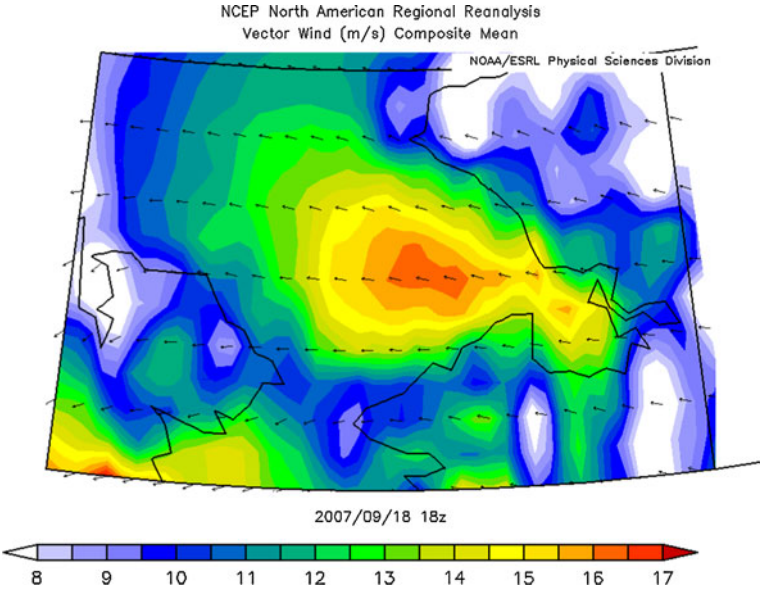

Fig. 12 SE1 vector wind composite. NARR 0.3° resolution 10-m wind showing magnitude and direction at September 18, 2007 1,800 UTC, 1 h before wave generation of highest SWH in SE1

direction bore almost no relationship to wave direction. On September 19, 0900, the local wind speed dropped from 16 to 8 m s^{-1} in 9 h. The wave height also decreased in a manner proportional to the wind speed, lagging by about 5 h. The wind and wave direction continued to coincide until September 20, 2100, when the wave direction rotated to a westerly orientation with a wave height of 1 m.

It was of interest to determine whether the NARR winds, as applied to a theoretical wave growth exercise, were able to reproduce the observed 3.7 m SWH that was shown for the wave spectrum. The time of propagation, t, in deep water is $t = 4\pi X/4(gT)$, where X is the fetch and T is the wave period. The available fetch X to the east of the RDCP was estimated at 175 km. The wave period T was 6.0 s. This resulted in a time of propagation t for the wave at 10 h. This would put the wave generation at September 18, 1900. According to the NARR 10-m wind field estimates, the maximum sustained easterly wind speeds of 16 m s^{-1} occurred around the beginning of this time at the RDCP location and throughout the Kotzebue Sound (see Fig. 12).

To summarize this section, it appears that the Bering Sea low in progress over 17–19 September played a major role in wave development during event SE1, generating moderate-to-strong local easterly winds that were of a magnitude not uncommon for this region. Driven by winds whose magnitude reached its highest state while wave height followed 2 h later at its highest state, a well-defined local-wave state developed, with easterly SWH exceeding 3 m for 16 h, which is classified as "wind-sea."

4.3 SE2 (SWH-3m-15), November 22–December 2, 2007 UTC

SE2 (SWH-3m-15) commenced on November 22, 2100 and ended December 2, 0800 (227 h' duration). In brief, the event proceeded as follows (Fig. 13): establishment of an

approximate 5-day period where SWH cycled between 1 and 2 m, then about 2 days at 2.5 m SWH, then an increase to a brief maximum 4 m SWH over a ~2-day period before a rapid decay ensued. The event began with a 1 m SWH with a westerly wave direction (Fig. 14) in which the direction lasted for 72 h (November 22, 2100–November 25, 2100). After this, a rapid change in wave direction to the east occurred; this direction persisted for the next one hundred and 50 h (November 25, 2100–December 2, 0300). However, unlike SE1 (SWH-3m-3), a sudden increase in wave height and period was not observed; rather, wave heights increased relatively gradually from 1 to 2 m over a 45-h period, and from 2 to 3 m over an additional 108-h period. A sustained 34-h period of easterly 3 m SWH was observed from November 30, 0900 to December 1, 1900; during this 3-m event, SWHs exceeded 4 m for 6 h (December 1, 0300–0900). After the 3-m event, the SWH decreased to 2 m and continued in the eastward direction for 8 h (December 1, 1900–December 2, 0300); then finally, the SWH decreased further to 1 m and wave direction changed around to southerly.

The synoptic situation during this period (Fig. 15) featured most prominently a low-pressure system that occurred over the Bering Sea from November 22–29, which was bordered to the east and northeast by an extensive, elongated high-pressure system stretching from the Gulf of Alaska to the Beaufort Sea, resulting in the highest wind speeds over the eastern Bering and southern Chukchi Seas. This storm, a classic stalled system, moved into the southwestern Bering Sea on November 22, north of the Andreanof Islands (US) and Near Islands (US) with an MSLP of 980 hPa supporting maximum winds at 925 hPa geopotential height of 18 m s^{-1}. Throughout the day of November 23, the storm rapidly intensified, dropping to an MSLP of 960 hPa, with the zone of maximum winds shifting around to a southeasterly direction blowing toward Kamchatka Peninsula (Russia) at 30 m s^{-1}. The low-pressure system moved slowly northwards over the Bering Sea before coming to rest north of Kamchatka Peninsula on December 1, 1500, at which point the storm had weakened to an MSLP of 980 hPa.

The "peak" of the storm occurred from November 27, 1200 to November 29, 1800 (54 h). Corresponding winds (925 hPa) during this time were southeasterly over the

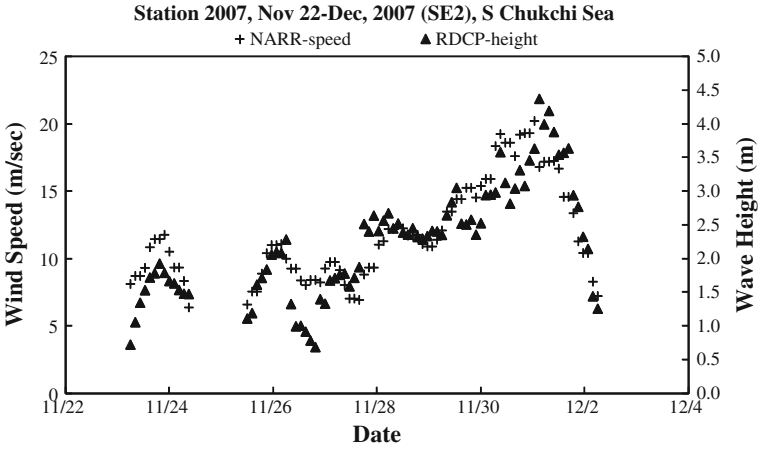

Fig. 13 SE2 wave height versus wind speed. Comparison of RDCP SWH and NARR 10-m wind speed at Station 2007 for wave record November 22–December 2, 2007 (SE2) at 67°3′29.94″N, 166°20′43.02″W, and with a water depth of 34 m

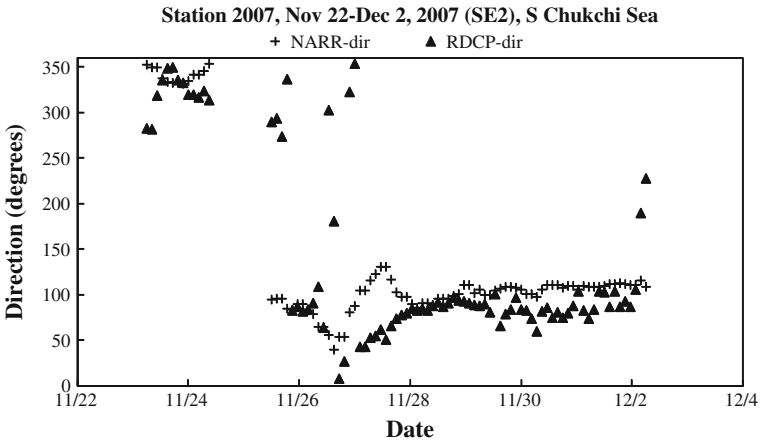

Fig. 14 SE2 wave direction versus wind direction. Comparison of RDCP mean wave direction and NARR 10-m wind direction at Station 2007 for wave record November 22–December 2, 2007 (SE2) at 67°3′29.94″N, 166°20′43.02″W, and with a water depth of 34 m

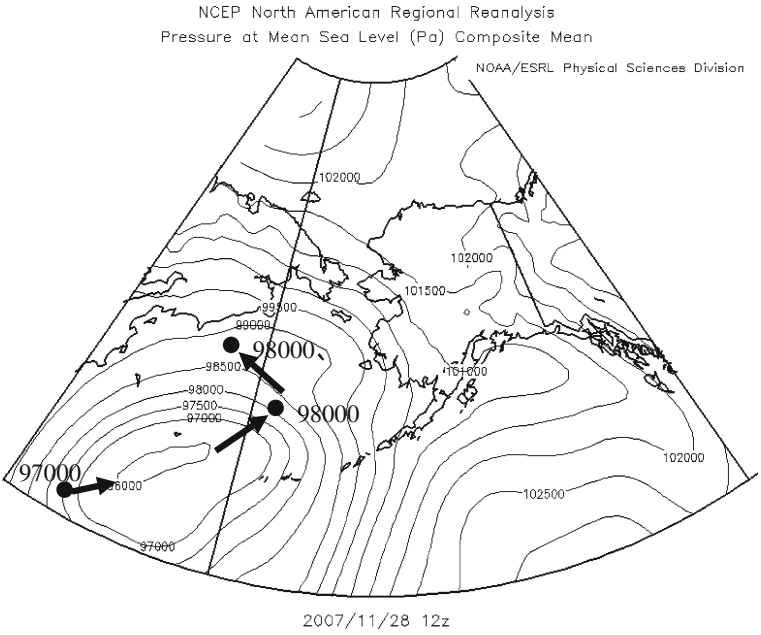

Fig. 15 SE 2 storm maxima. Storm maxima during SE2 on November 28, 2007 1,200 UTC shown on (NARR, MSLP) map. Image provided by the NOAA-ESRL Physical Sciences Division, Boulder Colorado at http://www.esrl.noaa.gov/psd. Modified by O. Francis, January 2011

Aleutians, Seward Peninsula, and southern Chukchi Sea, reaching speeds of 35 m s^{-1}. MSLP reached a minimum of 960 hPa for 42 h from November 27, 1500 to November 29, 0900; the center of the low was positioned between the Near Islands and the Andreanof

Islands, moving slowly northward toward Bering Strait. The drop in MSLP on November 27 immediately preceded the more active phase of SE2.

Figure 16 shows the wave spectrum at the highest SWH during December 1, 0300, which was 3 days after the peak storm period in the Bering Sea (November 28) and several hours after the peak wind of 20 m s^{-1} in the SE Chukchi Sea (November 30). The color bar (top) and non-directional (bottom) give the wave energy density, $E(f)$, in m^2Hz^{-1}. The Cartesian contour plot (Fig. 16) shows that the spectra range from 0.10 to 0.15 Hz and a 90° direction range for $E(f) > 2m^2Hz^{-1}$, similar to SE1. The non-directional peak energy density was 21.0 m^2Hz^{-1} (Fig. 13—bottom) at 0.12 Hz, while the directional (Fig. 13—top) was centered at 0.14 Hz coming from 83° (East). The integral wave parameter estimates derived from the spectra result in a SWH = 4.4 m, $T_{m02} = 6.3$ s, $T_{m01} = 6.5$ s. The mean winds during the period of the spectrum included a wind speed of $U_{10} = 16.8$ m s^{-1} and a wind direction of $U_{\text{dir}} = 110°$. Wind and wave direction were easterly, where wave direction (83°) was 27° counterclockwise from wind direction (110°). This was different compared to what was seen in SE1, where wave direction was clockwise to wind direction. The wind speed (16.8 m s^{-1}) was again greater than the wave phase speed. Since the wind speed was much greater than the wave phase speed, this strongly indicates a locally generated easterly "wind-sea" for the event of December 1, 0300.

Similar to SE1, the largest SWH represented wind-seas with some of the 1 m SWH clearly uncorrelated to the wind direction and presumably representing swell energy derived from a distant source. During the first part of SE2, winds were predominantly northwesterly and then change to easterly as the stronger southeast winds from the storm build into the Seward Peninsula area. Beginning November 22, 2100, a northwesterly wave of 1 m SWH commenced. Although the wave direction was coincident to the local wind direction, the wind magnitude—3 m s^{-1}—was not strong enough to develop the observed 1 + m sea, indicating swell propagating in from the broader Chukchi Sea. The wind direction changed to easterly on November 24, 1800, while the wave direction did not change to easterly until 27 h later on November 25, 2100. At this time, wave height and period increased from 1 to 2 m SWH and 4 to 5 s, respectively. Wind speed also increased from 8 to 10 m s^{-1}. During the 27-h period, while wind and wave direction were not similar, wind speed increased from 5 to 10 m s^{-1}.

SE2 wave heights are shown to be affected by prior wind events. On December 1, 0300, the local wind speed dropped from 20 to 17 m s^{-1} in 3 h, during the start of the 4 m SWHs. The 4 m SWHs lasted 6.75 h, and the 3 m SWH continued on for 9 h after the end of the 4 m SWH. Prior to the 4 m SWH event, the local wind speed was approximately 20 m s^{-1} for 20 h. The wind speed dropped to 16 m s^{-1} during the 17 h while the 4 and 3 m SWH events were happening. This was also assessed by using the wave parameters that occurred in the wave spectra (Fig. 16). The exercise whereby NARR winds are used to reproduce the event peak was repeated for SE2 for the observed 4.4 m SWH that was shown for the wave spectrum. Using time of propagation $t = 4\pi X/(gT)$ where X is the fetch at 180 km and T is the wave period at 6.5 s, this resulted in a $t = 10$ h. This would put the wave generation at November 30, 1700. According to the NARR 10-m wind field estimates, the highest wind speed values (+19 m s^{-1}) at the RDCP location and in the Kotzebue Sound (see Fig. 17) occurred during this time for SE2. This in turn yielded the highest wave height, recorded by the RDCP for SE2.

It appears that synoptic-scale low-pressure and a neighboring high-pressure system lasting for several days caused high wind speeds over the eastern Bering Sea and southern Chukchi Sea that drove the wave conditions observed during SE2. Unlike SE1, which saw

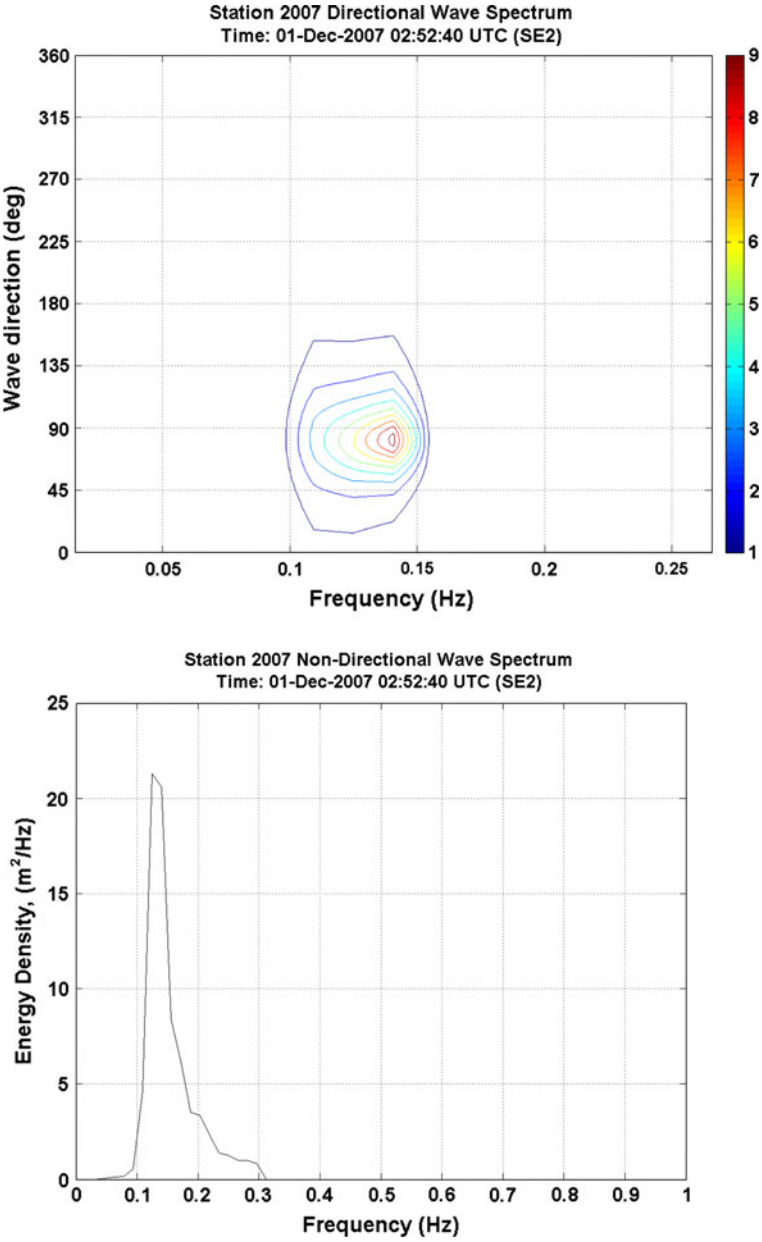

Fig. 16 SE2 wave spectrum. Directional (*top*) and non-directional (*bottom*) wave spectra Cartesian projection of highest SWH in SE2 on December 1, 2007 0,252 UTC during SE2, SWH = 4.4 m recorded by the RDCP at Station 2007 at 67°3′29.94″N, 166°20′43.02″W with a water depth of 34 m. *The color bar* (*top*) and non-directional (*bottom*) give the wave energy density, $E(f)$, in m^2Hz^{-1}

a well-defined local-wave state develop within 9 h, SE2 developed after 117 h where easterly SWH exceeding 3 m for 34 h and reached over 4 m for 6 h. Similar to SE1, SE2 was also classified as "wind-sea".

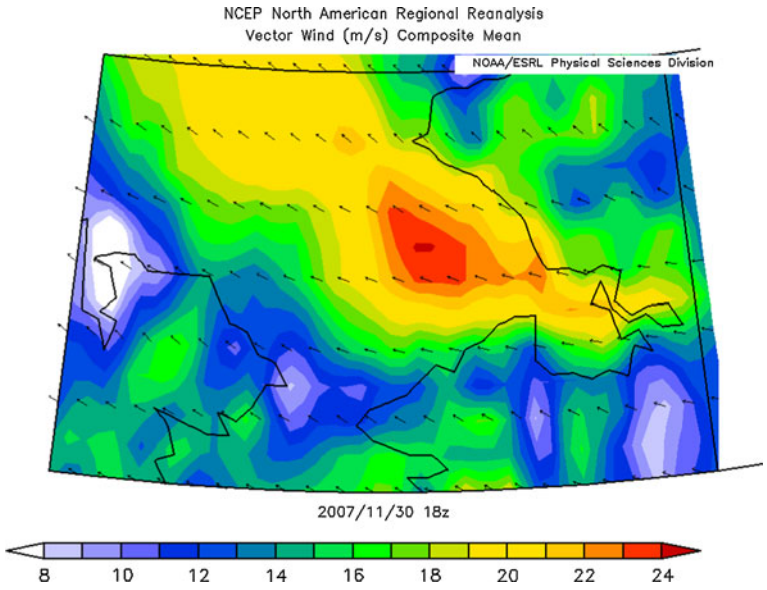

Fig. 17 SE2 vector wind composite. NARR 0.3° resolution 10-m wind showing magnitude and direction at November 30, 2007 1,700 UTC, 1 h after wave generation of highest SWH in SE2

5 Conclusion

SWHs exceeding 2 m observed by the RDCP in the SE Chukchi Sea in the fall of 2007 appeared to be locally generated wind-sea and not derived from distant energy sources typically suggesting swell. The primary support for this is the observation that, for the two 3 m SWH events, wind and wave directions during the event peak were easterly, with wind/wave direction exhibiting strong phase locking.

Wave direction was opposite of the current flow direction, however. There is a strong current prominent in the southeast Chukchi Sea region, traveling eastward (Coachman and Tripp 1970; Overland and Roach 1987; Woodgate et al. 2005; Panteleev et al. 2010) over the Station 2007 area. This was thought to be due to the influence of a strong "wind-sea" seen for the higher SWHs (<2 m). The lower SWHs (<1 m) showed a westerly wave direction, the same direction that the current over Station 2007 also flows. Therefore, current flow from the west that is present at Station 2007 was overcome by the strong easterly winds, which caused the wave state to become easterly, creating an easterly "wind-sea".

It is apparent that the available fetch from the Kotzebue Sound was sufficient to generate large waves over Station 2007. It is suggested that observed wave states are dependent on fetch and not just wind magnitude, since the NARR reanalysis data set showed that the boundary of the generating wind field lay in the proximity of what was estimated in this study when using variables known such as wave period and time of propagation. Winds from the NARR reanalysis data set were also shown to adequately provide the wind forcing needed for the observed wind-sea states.

Given the orientation of the Sound, it is not clear that northeast and southeast fetch directions, which are more constrained than fetches aligned more due to east as well as to most westerly directions, would be able to sustain similar SWH under similar wind speeds.

However, a key point for the offshore southeast Chukchi Sea region (i.e., region around Station 2007) is that, unlike farther more southern regions, storms often stall and when they do they are often positioned over the eastern Bering Sea. A stalled weather pattern allows wind duration to be maximized, which allows a given wind magnitude to reach fully developed sea state for the given fetch. This is important because, for this fetch-limited region, if a storm does not stall, a fully developed sea state is unlikely to be attained, and, with maximum wind speeds rarely exceeding 40 m s^{-1}, waves exceeding 2 m are unlikely to occur otherwise.

The wave-state potential for this region has been demonstrated to be capable of supporting a SWH of 4 m and extended storm durations of +3 m SWH. An easterly wind and thus wave direction would impact the main shipping route through the Bering Strait and could hamper operations, resulting in delays. Examples of operations in the Bering Strait include Coast Guard vessels, oil lease support vessels, and drilling activity, the bulk carriers that travel to and from the Teck Alaska Inc. Delong Mountain Terminal, along with local small craft from various coastal communities. It is anticipated with the reduction in the Arctic ice pack, an increasing quantity of traffic moving through the area will increase. Any developers of offshore structures, such as jack-up rigs or artificial production islands, must factor sea states of at least this magnitude into design considerations and must assume that they will occur annually, given the frequency of storms and of stalled storms that occur in the Bering Sea region.

Acknowledgments This publication is the result in part of research sponsored by the Cooperative Institute for Arctic Research (CIFAR) with funds from the NOAA under cooperative agreement NA17RJ1224 with the University of Alaska. Funding was also provided by NOAA projects, NA06OAR4600179 and NA08OAR4600856. Generous logistical support from Teck Alaska Incorporated and Foss Maritime Company has been provided to this project from its beginning.

References

AADI (Aanderaa Data Instruments) (2006) RDCP primer TD 220c, 70 pp

Coachman LK, Tripp RB (1970) Currents north of Bering Strait in winter. Limnol Oceanogr 15(4):625–632

Ewing JA (1980) Observations of wind-waves and swell at an exposed coastal location. Estuar Coast Mar Sci 10:543–554

Francis-Chythlook O (2004) Coastal processes in Elson Lagoon, Barrow, Alaska. MS Thesis, University of Alaska Anchorage, Anchorage

Francis OP, Panteleev GG, Atkinson DE (2011) Ocean wave conditions in the Chukchi Sea from satellite and in situ observations. Geophys Res Lett 38:L24610. doi: 10.1029/2011GL049839

Francis OP, Atkinson DE (2012) Synoptic forcing of wave state in the southeast Chukchi Sea, Alaska, at nearshore locations. Nat Hazards. doi: 10.1007/s11069-012-0148-y

Hudak DR, Young JMC (2002) Storm climatology of the southern Beaufort Sea. Atmos Ocean 40:145–158

Jensen R, Scheffner N, Smith SJ, Webb D, Ebersole B (2002) Engineering studies in support of delong mountain terminal project ERDC/CHL TR-02-26, Vicksburg, MS

Kistler R, Kalnay E, Collins W, Saha S, White G, Woollen J, Chelliah M, Ebisuzaki W, Kanamitsu M, Kousky V, van den Dool H, Jenne R, Fiorino M (2001) The NCEP-NCAR 50-year reanalysis: monthly means CD-ROM and documentation. Bull Amer Meteor Soc 82:247–267

Mesinger F, DiMego G, Kalnay E, Mitchell K, Shafran PC, Ebisuzaki W, Jovic D, Woollen J, Rogers E, Berbery EH, Ek MB, Fan Y, Grumbine R, Higgins W, Li H, Lin Y, Manikin G, Parrish D, Shi W (2006) North American regional reanalysis. Boulder, CO NOAA.OAR/ESRL PSD:42

Mesquita MDS, Atkinson DE, Hodges KI (2010) Characteristics and variability of storm tracks in the North Pacific, Bering Sea, and Alaska. J Clim 23:294–311. doi:10.1175/2009JCLI3019.1

Overland JE, Roach AT (1987) Northward flow in the Bering and Chukchi Seas. J Geophys Res 92(C7):7097–7105

Panteleev G, Nechaev DA, Proshutinsky A, Woodgate R, Zhang J (2010) Reconstruction and analysis of the Chukchi Sea circulation in 1990–1991. J Geophys Res 115:C08023. doi:10.1029/2009JC005453

Swail VR, Cox AT (2000) On the use of NCEP–NCAR reanalysis surface marine wind fields for a long-term North Atlantic wave hindcast. J Atmos Ocean Technol 17:532–545

USACE (2003) Kivalina relocation planning project inventory and village requirements, Kivalina, Alaska. Prepared by Tryck Nyman Hayes, Inc. for US Army Corps of Engineers, Alaska District

USACE (2004) Kivalina relocation master plan, Kivalina, Alaska. Prepared by Tryck Nyman Hayes, Inc. for US Army Corps of Engineers, Alaska District

WMO (World Meteorological Organization) (1998) Guide to wave analysis and forecasting, 2nd edn. WMO-No. 702, Secretariat of the World Meteorological Organization, Geneva. ISBN 92-63-12702-6, 159 pp

Woodgate RA, Aagaard K, Weingartner T (2005) A year in the physical oceanography of the Chukchi Sea: moored measurements from autumn 1990–91. Deep Sea Res Part II 52(24–26):3116–3149